Article ID: 1000-324X(2016)06-0661-06 **DOI:** 10.15541/jim20150579

Effect of Residual Phase and Grain Size on Corrosion Resistance of SiC Ceramics in Mixed HF-HNO_3 Acid Solution

LIU Ze-Hua[1, 2], QI Qian[2], YAN Yong-Jie[2], ZHANG Hui[2], LIU Xue-Jian[2], LUO Hong-Jie[1], HUANG Zheng-Ren[2]

(1. School of Materials Science and Engineering, Shanghai University, Shanghai 200444, China; 2. State Key Laboratory of High Performance Ceramics and Superfine Microstructure, Shanghai Institute of Ceramics, Chinese Academy of Sciences, Shanghai 200050, China)

Abstract: Effect of residual phase and grain size the corrosion resistance of SiC ceramics in mixed HF-HNO_3 acid solution was investigated. Three kinds of fabrication methods (SSiC–solid state sintered SiC, LPS SiC–liquid phase sintered SiC and RB SiC–reaction bonded SiC) were adopted to prepare SiC ceramics. Besides, the grain size in SiC ceramics was adjusted under different sinter temperatures. Compared to RB SiC and LPS SiC ceramics, SSiC ceramics showed a better corrosion resistance for the good corrosion resistance of residual graphite and 'island' structure of residual phase in ceramics. The grain size of SiC ceramics sintered at temperature between 2100℃ and 2160℃ increase from 2 μm to 6 μm, and the absolute values of *Y* intercept, which reflect the corrosion of SSiC ceramics with none residual phase, are 9.22 μg/cm^2 (2100℃), 5.81 μg/cm^2 (2130℃) and 0.29 μg/cm^2 (2160℃), which demonstrate that large grain size is beneficial to the corrosion resistance of SiC ceramics.

Key words: SiC; corrosion resistance; residual phase; grain size

Silicon carbide (SiC) ceramic materials and their composites with excellent chemical stability, superior high-temperature mechanical properties, outstanding corrosion resistance, have been widely used in the aggressive environments, such as parts of engines and aerospace vehicles, bearing and seeding in chemical equipment. Despite of the excellent chemical stability of SiC ceramics at room temperature, corrosion still exists in corrosion environments. Moreover, the corrosion rate can be fast, when the ceramics are applied in superficial aggressive environment, such as the pressurized water reactors. In recent studies, researchers found that the concentration and temperature of the corrosion solution and the residual phase in grain boundary had effects on the corrosion resistance of ceramics in acid and basic aqueous solutions[1-4]. Hirayama, *et al*[5] found that the dissolution rate of SSiC followed linear kinetics in an oxygenated alkaline solution, whereas it approximated parabolic kinetics in acid solution. The investigation of Kim, *et al*[6-7] revealed that the corrosion resistance of SiC ceramics in high temperature water greatly depended on the fabrication methods of SiC. Andrews, *et al*[8] used electrochemical method to investigate the corrosion behavior of LPS SiC and SSiC ceramics in acid and alkaline solution, finding that C in SSiC could not be corroded in acid or alkaline solution and the corrosion rate of LPS SiC grain were more than an order of magnitude lower than that observed in SSiC. Sydow, *et al*[9] found that the electrochemical corrosion resistance of the LPS SiC ceramics was instigative affected by the core-rim structure of LPS SiC ceramics in acid and alkaline solutions. Herrmann, et al[10] studied the electrochemical corrosion resistance of SSiC, suggesting that the corrosion resistance of specimens was strong influenced by the formation of SiO_2 layer. Medvedovski, *et al*[11] investigated the corrosion behavior of high alumina ceramics, finding that the grain size had a significant effect on the strength and corrosion resistance and as the grain size increased, the strength and corrosion decreased. However, there is little investigation on the effect of residual phase and grain size on the corrosion resistance of SiC ceramics in a mixed acid solution at elevated temperature.

In this paper, SSiC with C and B_4C as sintering aids, LPS SiC with Y_2O_3 and Al_2O_3 as sintering aids and RB SiC were prepared to study the relationship between the residual phase and corrosion resistance. SSiC ceramics sintered at different temperature were prepared to investi-

Received date: 2015-11-24; **Modified date:** 2016-01-24
Foundation item: National Natural Science Foundation of China (51202270); Strategic Pilot of Science and Technology of Chinese Academy of Sciences (Class A: XDA02040206)
Biography: LIU Ze-Hua(1989–), male, candidate of master degree. E-mail: liuzehualxtx@126.com
Corresponding author: HUANG Zheng-Ren, professor. E-mail: zhrhuang@mail.sic.ac.cn

gate the effects of grain size on the corrosion resistance of specimens. The waste acid came from wafer in semiconductor fabrication and stainless steel manufacturing often contains mixed acid solution (HF and HNO_3), and a high temperature is needed to recycle the mixed acid. To simulate the application environment, the mixed acid solution (HF and HNO_3) at elevated temperature was chosen as the corrosion medium.

1 Experimental procedure

1.1 Specimen Preparation

In the corrosion test, LPS SiC, RB SiC and SSiC ceramics were used as the sample.

A green sample was produced by adding a certain amount of SiC powder, polyvinyl butyral (PVB) solution of 1wt%, with an additional C (5wt%, 6wt%, 7wt%, 8wt%) and 0.6wt% B_4C were introduced as sintering additives. The powders were mixed and milled in ethanol with SiC balls for 24 h and then dried with a rotary evaporator is vacuum at 60℃. The SSiC green powders were first uniaxial dry pressed at 60 MPa, followed by cold isostatic pressing at 200 MPa for 120 s. The green specimens of SSiC were heated to 900℃ for 1 h in vacuum to remove the binder. After binder removal, the samples were sintered at different temperatures (2100℃, 2130℃, and 2160℃) for 2 h in argon at a heating rate of 10℃/min.

The green specimens of LPS SiC with 3.01wt% Al_2O_3 and 3.99wt% Y_2O_3 as sintering aids were prepared like SSiC. After the same process of binder removal, the specimen were heated to 1600℃ at heating rate of 10℃/min, following by heating rate of 2℃/min up to the sintered temperature 1930℃, at which they were kept for 1 h.

In the same way of SSiC, The green specimens of RB SiC were also prepared, while with the raw materials of SiC powders with 5 μm and 50 μm and C with the content of 45:45:10 in weight. Then the green specimens were sintered in vacuum with access Si particles surrounded at 1750℃ for 2 h at a heating rate of 5℃/min.

All the heat-treatment processes were carried out in a high-temperature graphite resistance furnace.

The composition and relative density of the samples were listed in table 1 and the relative density of SSiC ceramics as shown in Fig. 1. The samples were cut into 3 mm× 4 mm×36 mm rectangular coupons and ϕ20 mm×3 mm wafers which were polished by diamond paste (grain size: 1 μm). The three-point bending strength was measured before and after corrosion test using the rectangular samples and the wafers were used to study the behavior and mechanism of corrosion. All specimens were cleaned three times with distilled water and ethanol, respectively. After dried at 120℃ for 12 h, the specimens were finally weighed on an analytic balance with a 0.1 mg resolution.

Table 1 Characteristics of the Samples

Specimen	Composition / wt%					Density/(g·cm^{-3})	Relative density/%
	Si	Al_2O_3	Y_2O_3	C	B_4C		
RB SiC	15.02	—	—	—	—	3.05	99.47
LPS SiC	—	3.01	3.99	—	—	3.29	99.32
SSiC	—	—	—	5	0.6	3.18	98.75

*SSiC sintered at 2130℃.

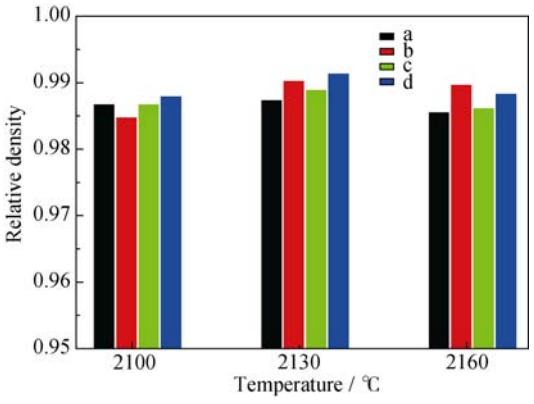

Fig. 1 The relative density of SSiC ceramics with different contents of C sintered at different temperatures
(a) 5wt% C; (b) 6wt%C; (c) 7wt% C; (d) 8wt% C

1.2 Corrosion procedure

Each group of the corrosion test, five bars and one polished wafer were immersed into the same mixed acid solution (V(HF):V(HNO_3)=1:2) in a 100 mL Teflon-lined stainless-steel autoclave. The corrosion tests of SiC ceramics were proceeded at 175℃ for 24 h (SSiC), 2 h (LPS SiC) and 0.5 h (RB SiC). The corrosion time was decided by the corrosion of ceramics. After corrosion, SiC grain could be detected and the mass loss of specimen would be measured.

1.3 Characterization

X-ray diffraction (XRD, Expectron XDC-1000, Jungner Instrument, Solna, Sweden) with Cu Kα radiation was used to identify the phase composition of the corroded

specimen. The surfaces and the cross-sections of specimen were examined using a scanning electron microscope (SEM, Hitachi TM3000, Japan).

2 Result and discussion

The possible corrosion reactions of SiC in the mixed acid solution are listed as follows:

$$SiC+8HNO_3\,(l)=CO\,(g)+8NO_2\,(g)+4H_2O\,(l)+SiO_2 \quad (1)$$

$$SiC+3/2O_2\,(g)=SiO_2+CO\,(g) \quad (2)$$

$$SiC+4HF\,(l)=SiF_4\,(g)+CH_4\,(g) \quad (3)$$

$$SiC+2H_2O\,(l)=SiO_2+CH_4\,(g) \quad (4)$$

$$SiC+3H_2O\,(l)=SiO_2+CO\,(g)+3H_2\,(g) \quad (5)$$

$$SiC+5H_2O\,(l)=Si(OH)_4\,(l)+CO\,(g)+3H_2\,(g) \quad (6)$$

$$SiO_2+4HF\,(l)=SiF_4\,(g)+2H_2O\,(l) \quad (7)$$

The residual phase in the grain boundary is also corroded in the corrosion medium. The possible corrosion reactions of residual phase in RB SiC ceramics are listed as follows.

$$Si+4HF\,(l)=SiF_4\,(g)+2H_2\,(g) \quad (8)$$

$$Si+O_2\,(g)=SiO_2 \quad (9)$$

The corrosion reactions, which can proceed only in SSiC in mixed acid solution, are listed.

$$C+2HNO_3\,(l)=CO\,(g)+2NO_2\,(g)+H_2O\,(l) \quad (10)$$

$$C+4HF\,(l)=CF_4\,(g)+2H_2\,(g) \quad (11)$$

$$C+H_2O\,(l)=CO\,(g)+H_2\,(g) \quad (12)$$

In LPS SiC, the possible corrosion reaction of residual phase are also listed as follows,

$$Y_3Al_5O_{12}+24H^+=3Y^{3+}+5A^{3+}+12H_2O \quad (13)$$

From the calculation results of the HSC Chemistry (6), the Free Gibbs energy of all reactions except reaction (9) and (10) is negative at 175℃, indicating that the reactions can occur spontaneously in corrosion medium theoretically. The calculation results of enthalpy show that reaction (1) and (2) need more energy. Andrews, *et al*[8] found the layer of SiO_2 was formed when SiC ceramics were immersed into HNO_3 solution by electrochemical method, suggesting that reaction (1) and (2) may proceed in solution. Kuang and Cao[12] investigated the oxidation behavior of SiC whisker, demonstrated that SiC oxidized very slowly below 1100℃ in air, implying that reaction (2) had little effect on the corrosion of SiC in this tests. Other reactions were confirmed by other researchers[13].

2.1 Residual phase

Due to the different corrosion resistance of residual phases, various corrosion time was designed to evaluate the mass loss was used to evaluate the corrosion resistant of different residual phase in SiC ceramics. Fig. 2(a) shows the mass loss of different types of SiC ceramics. Comparing to SSiC, the RB SiC and LPS SiC corrode quickly in this environment. The mass loss of RB SiC and LPS SiC is 236.37 μg/cm^2 and 8.79 μg/cm^2, respectively, while they are below 0.57 μg/cm^2 for SSiC ceramics, revealing that the residual Si and $Y_3Al_5O_{12}$ are corroded easier than C in the mixed acid solution, which also can be verified by the microstructure observation. XRD patterns of different specimens before and after corrosion are shown in Fig. 2(b)-(d). In RB SiC specimens, the intensity of the Si phase significantly decreased, indicating that most Si phase dissolved into the solution in Fig. 2(b). The intensity of $Y_3Al_5O_2$ (YAG) phases in LPS SiC reduced, as shown in Fig. 2(c), which demonstrates that the residual phase in grain boundary leads to the mass loss. From the Fig. 2(d), it can be seen that no obvious change is found, implying that the residual phase corroded little in those solutions. Therefore, the residual phase in grain boundary is the main factor to cause the mass loss based on the XRD patterns. From the analysis of chemistry reactions above, SiO_2 should exist in the surface of specimens. However, we cannot find it in Fig. 2(b)-(d), and the reason is that the amount of SiO_2 formed by corrosion is slight, and the SiO_2 can be corroded by HF and dissolve in the corrosion medium during the corrosion time.

The corrosion resistance of samples with different content of residual phases was investigated to discuss the effect of the residual phase on the corrosion behaviors. Fig. 3(a) shows the mass loss is in proportion to the content of C in corrosion solution, which suggests that the residual C is corroded in corrosion medium. Since the corrosion of specimens in corrosion medium is consist of two parts: the corrosion of residual phase and the corrosion of SiC. Because of the low the active energy in grain boundary, SiC grains could be measured by the micrograph of corroded specimen in Fig. 3(b). As the content of C increased, the grain size decreased which was proved by Stobierski, *et al*[14]. As the grain size decrease, grain boundary increase. Then the mass loss enlarges and the slope of fitting linear change. The absolute value of *Y* intercept of fitting linear can be used to simulate the mass loss of specimens with no residual phase, so it is used to reflect the corrosion of SiC grain.

The microstructures of different SiC specimens before and after the corrosion are shown in Fig. 4. Though all corrosion reactions mainly proceeded in the grain boundary, the micrographs of corroded specimens are different for the different residual phases in grain boundary. In the micrographs of corroded SSiC, pores and grain boundary were found, but the grains contact with each other, while the grains are separated by the gaps in LPS SiC and RB SiC ceramics. In the LPS SiC and RB SiC specimens, the residual phase could form a network structure, and the corrosion reaction could proceed continuous, which lead

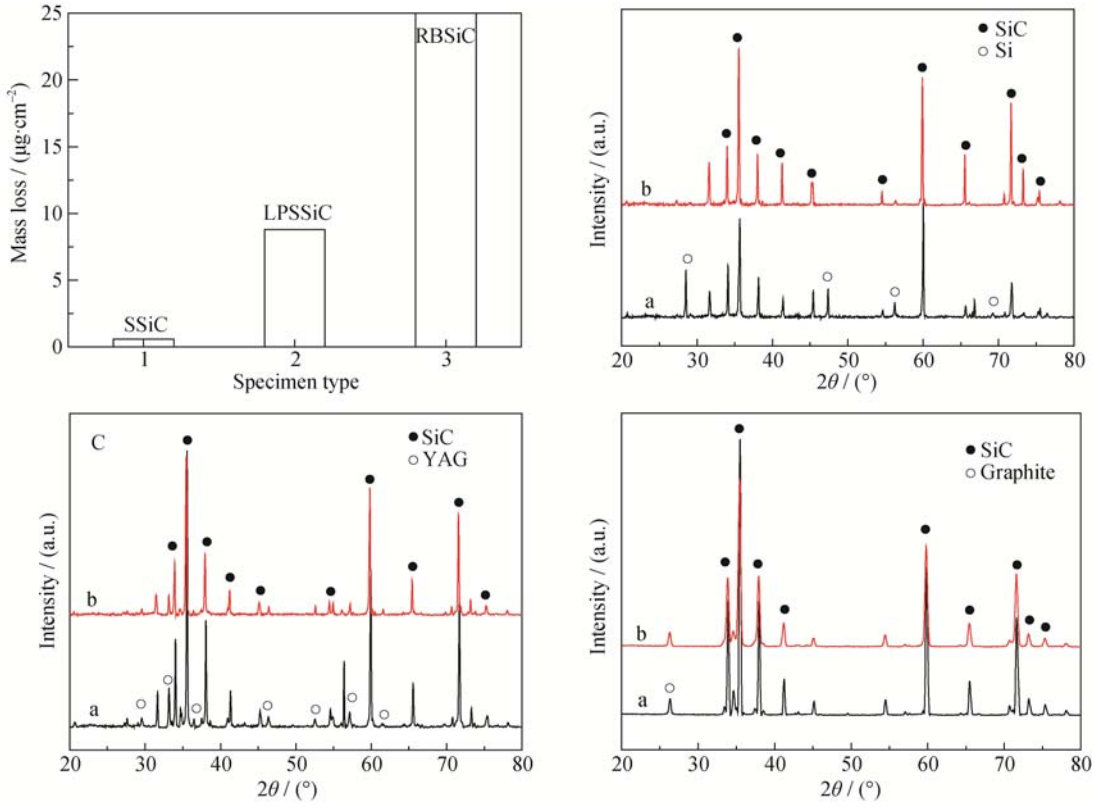

Fig. 2 The mass loss of different type SSiC ceramics (a), XRD patterns (b-d) of different SiC ceramics before and after corrosion. RB SiC (b), LPS SiC (c) and SSiC with 8wt% C (d)

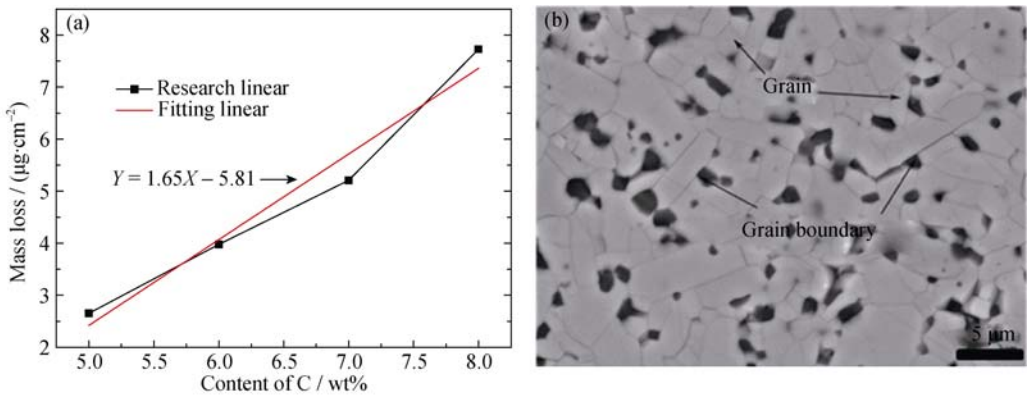

Fig. 3 Mass loss *versus* the content of residual phase (a) and cross-sectional micrograph of corroded SSiC with 5wt% C sintered at 2130℃ (b)

to the drop of grains surrounded by residual phase from the ceramics easily. While SiC grain divides the residual phase in SSiC, the internal residual phase cannot be corroded, and the corrosion intensity is very slight.

2.2 Grain size

Based on the discussion above, SSiC specimens exhibited good corrosion resistance for the dispersed distribution of residual phase. It can be easily understood that the place with high energy, such as grain boundary and defect, can be corroded first by the corrosion medium. The grain boundary can be altered by changing the grain size, which is controlled by the sintered temperature. In this research, different sintered temperature is adopted to control the grain size. Fig. 4(a) shows the mass loss of specimens with different contents of C sintered at different temperature. In the same sintered temperature, the mass loss enlarged as the content of C increased, which could be explained by the corrosion of residual C in the solution. The corrosion resistance of specimen with same C content sintered at higher temperature was better than specimens sintered at lower temperature, indicating that the main factor influencing the corrosion is the grain boundary. In Fig. 4(a), the mass loss of specimen with 6wt% C sintered at 216℃ is abnormal, which attributes to the non-uniform

distribution of C in specimen, and the value is abandoned in Fig. 4(c). Because the corrosion reactions proceed at grain boundary, SiC grain is found and the grain size increase from 2 μm (2100℃) to 6 μm (2160℃) in Fig. 4(d)-(f). The grain boundary is harder to be found when the sintered temperature is 2160℃ than the sintered temperature is 2100℃, indicating that the specimens sintered at 2160℃ is more difficult to be corroded. In Fig. 4(b) and Fig. 4(c), the absolute value of *Y* intercept reduce from 9.22 μg/cm^2 to 0.29 μg/cm^2, when the sintered temperature increases from 2100℃to 2160℃, implying that the grain boundary reduce as the sintered temperature increase.

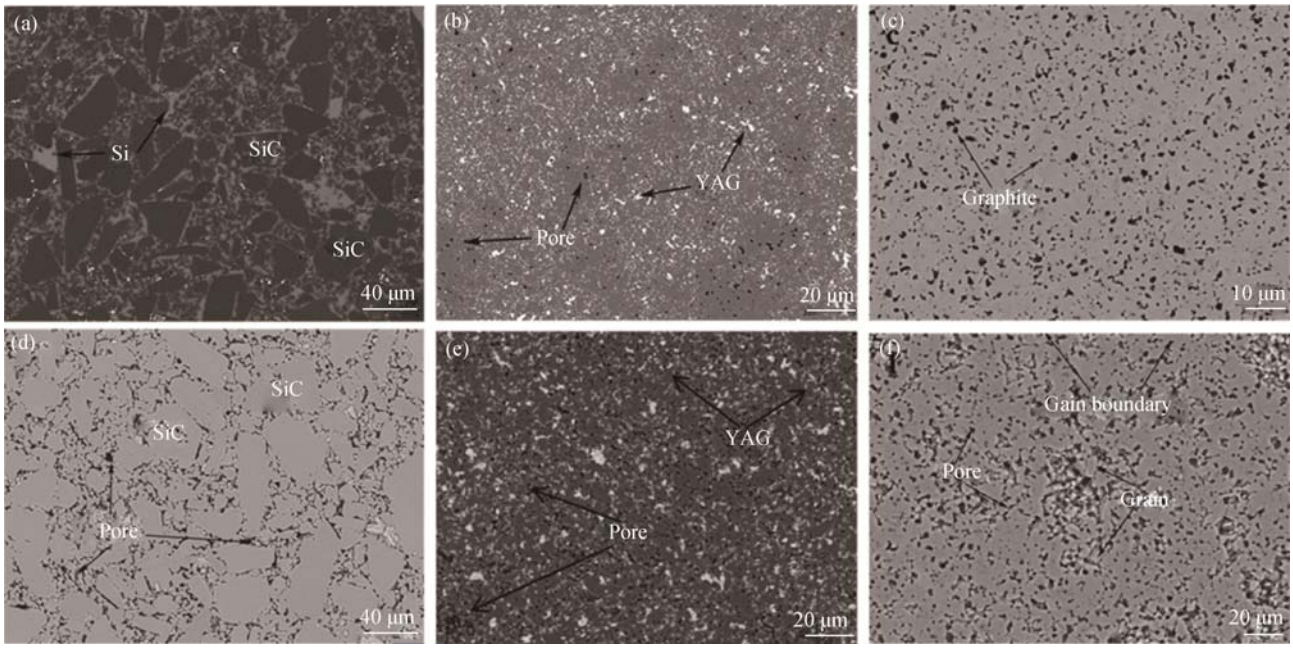

Fig. 4　SEM micrographs of the surface for different SiC ceramics
Before corrosion: (a) RB SiC; (b) LPS SiC; (c) SSiC
After corrosion: (d) RB SiC; (e) LPS SiC; (f) SSiC

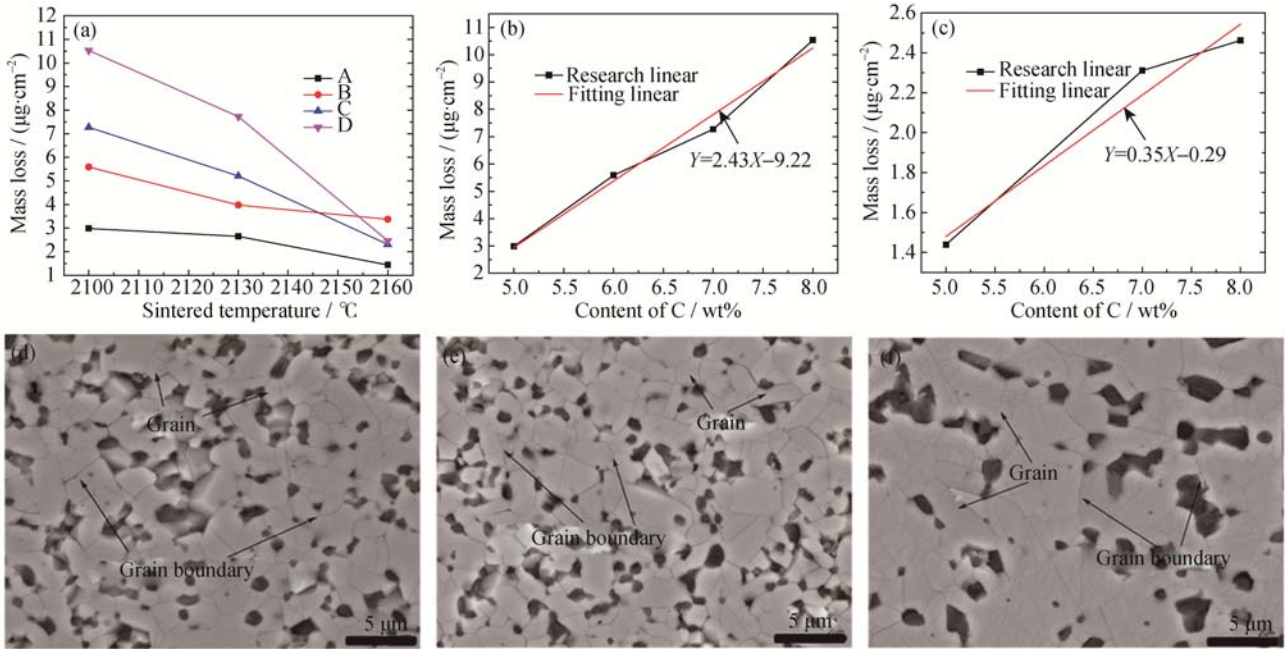

Fig. 5　Mass loss of SSiC with different contents of C *versus* sintering temperatures (a): A 5wt%C, B 6wt %C, C 7wt %C and D 8wt%C. The mass loss *versus* the content of residual phase of SSiC sintered at different temperatures: (b) 2100℃; (c) 2160℃. SEM micrographs of surface for different corroded specimens with 5wt% C sintered at different temperatures: (d) 2100℃; (e) 2130℃; (f) 2160℃

3 Conclusion

In this paper, the effect of residual phase and grain size on the corrosion resistance of SiC ceramics in mixed HF-HNO_3 acid was studied. Three kinds of fabricate methods were used to prepare SiC ceramics with different residual phases, and the mass loss was used to estimate the corrosion resistance of different specimens. Due to the corrosion resistance of residual phase and the structural of residual C, SSiC ceramics exhibits a better corrosion resistance than LPS SiC ceramics with YAG and RB SiC with Si. Moreover, because of the different of corrosion resistance between SiC grain and residual phase, SSiC ceramics with the least C get the best corrosion resistance. Besides, the grain size of SiC also shows significant influence on the corrosion resistance of SSiC ceramics, The grain size increases from 2 μm to 6 μm as the sintered temperature improves from 2100℃ to 2160℃. From the corrosion results of SSiC sintered at different temperatures, SSiC ceramics sintered at higher temperature exhibit a better corrosion resistance for enlarging grain boundary.

References:

[1] SCHILM J, GRUNER W, HERRMANN M, *et al*. Corrosion of Si_3N_4-ceramics in aqueous solutions, Part I: Characterization of starting materials and corrosion in 1N H_2SO_4. *J. Eur. Ceram. Soc.*, 2006, **26(16):** 3909–3917.

[2] SCHILM J, GRUNER W, HERRMANN M, *et al*. Corrosion of Si_3N_4-ceramics in aqueous solutions. Part II: Corrosion mechanisms in acids as a function of concentration, temperature and composition. *J. Eur. Ceram. Soc.*, 2007, **27(12):** 3573–3588.

[3] SCHILM J, HERRMANN M, MICHAEL G, *et al* Leaching behavior of silicon nitride materials in sulphuric acid contained KF. *J. Eur. Ceram. Soc.*, 2004, **24(8):** 2319–2327.

[4] SPEIPEL B, NICKEL G K. Corrosion of silicon nitride in aqueous acidic solutions: penetration monitoring. *J. Eur. Ceram. Soc.*, 2003, **23(4):** 595–602.

[5] HIRAYAMA H, KAWAKUBO TAKASHI, GOTO AKIRA, *et al*. Corrosion behavior of silicon carbide in 290℃ water. *J. Am. Ceram. Soc.*, 1989, **72(11):** 2049–2053.

[6] KIM J W, HWANG S H, PARK Y J. Corrosion behavior of reaction-bonded silicon carbide ceramics in high-temperature water. *J. Mater. Sci. Lett.*, 2002, **21(9):** 733-735.

[7] KIM J W, HWANG S H, PARK Y J. Corrosion behavior of sintered and chemically vapors deposed silicon carbide ceramics in water at 360℃. *J. Mater. Sci. Lett.*, 2003, **22(8):** 581–584.

[8] ANDREWS A, HERRMANN M, SEPHTON M, *et al*. Electrochemical corrosion of solid and liquid phase sintered silicon carbide in acidic and alkaline environments. *J. Eur. Ceram. Soc.*, 2007, **27(5):** 2127–2135.

[9] SYDOW U, SEMPF K, HERRMANN M, *et al*. Electrochemical corrosion of liquid phase sintered silicon carbide ceramics. *Mater. Corros.*, 2013, **64(3):** 218-224.

[10] HERRMANN M, SEMPF K, SCHNEIDER M, *et al*. Electrochemical corrosion of silicon carbide ceramics in H_2SO_4. *J. Eur. Ceram. Soc.*, 2014, **34(2):** 229–235.

[11] EUGENE MEDVEDOVSKI. Influence of corrosion and mechanical loads on advanced ceramic components. *Ceram. Int.*, 2013, **39(3):** 2723–2741.

[12] KUANG J L, CAO W B. Oxidation behavior of SiC whiskers at 600-1400℃ in air. *J. Am. Ceram. Soc.*, 2014, **97(9):** 2698–2670.

[13] BARRINGER E, FAIZTOMPKINS Z, FEINROTH H. Corrosion of CVD silicon carbide in 500℃ supercritical water. *J. Am. Ceram. Soc.*, 2007, **90(1):** 315–318.

[14] STOBIERSKI L, GUBEMAT A. Sintering of silicon carbide I: Effect of carbon. *Ceram. Int.*, 2003, **29(2):** 287–292.

残余相和烧结温度对碳化硅陶瓷抗混酸腐蚀特性的影响

刘泽华[1,2], 齐 倩[2], 闫永杰[2], 张 辉[2], 刘学建[2], 罗宏杰[1], 黄政仁[2]

(1. 上海大学 材料科学与工程学院, 上海 200444; 2. 中国科学院 上海硅酸盐研究所, 高性能陶瓷和超微结构国家重点实验室, 上海 200050)

摘 要: 本工作主要研究了残余相和晶粒尺寸对碳化硅的抗混酸(HF-HNO_3)腐蚀特性。通过不同的烧结方法(固相烧结、液相烧结、反应烧结)制备出残余相不同的碳化硅材料。结果表明: 与液相烧结碳化硅(LPS SiC)和反应烧结碳化硅(RB SiC)相比, 固相烧结碳化硅(SSiC)具有更好的腐蚀抗性, 这是由于残余相石墨的抗腐蚀性强, 以及残余相在材料中形成不能相互联通的岛状结构。通过调节碳化硅的烧结温度, 可以影响材料中的晶粒尺寸, 研究结果发现相同烧结温度下随着残余相含量的增加, 材料腐蚀失重线性增加, 对曲线进行线性拟合, 其 Y 轴截距的绝对值代表不含碳的试样在该烧结温度下的腐蚀失重。研究表明随着烧结温度由 2100℃升高到 2160℃, 晶粒尺寸由 2 μm 增加到 6 μm。此时其 Y 轴截距的绝对值分别为 9.22(2100℃), 5.81(2130℃), 0.29(2160℃), 表明晶粒尺寸的增加有利于提高材料的抗腐蚀能力。

关 键 词: 碳化硅; 抗腐蚀; 残余相; 晶粒尺寸

中图分类号: TQ174 **文献标识码:** A